Indian Journal of Pure & Applied Physics
Vol. 61, September 2023, pp. 778-780
DOI: 10.56042/ijpap.v61i9.3841

Dielectric Study of Ytterbium Doped $ZnFe_2O_4$ Spinel Ferrite Synthesized by Solution Combustion Method

Laxmikant Banaj & Sadhana Agrawal*

Department of Physics, National Institute of Technology, Raipur 492 010, India

Received 15 July 2023; accepted 11 August 2023

A series of $ZnFe_2O_4$ spinel ferrite doped with Ytterbium ions were synthesized using the solution combustion method. The XRD patterns of the prepared samples confirmed the cubic spinel structure with space group Fd-3m. Scherrer's formula was used to calculate the crystallite size of the samples and it was found to be 20.69, 17.16 and11.09 nm. The SEM image showed irregular morphological distribution. The Dielectric constant and dielectric loss were studied at different temperatures and frequencies. The impedance analysis indicates that the conduction mechanism depends highly on the grain boundary resistance.

Keywords: Spinel ferrite; Dielectric constant; Dielectric loss; Impedance analysis

1 Introduction

Ferrites are promising ceramics having applications in microwave, biomedical, high-frequency devices etc. The spinel ferrite's general formula is AFe_2O_4, where A represents divalent cations and Fe represents trivalent cations in tetrahedral and octahedral sites respectively. Spinel ferrite materials are classified as normal, inverse, and mixed spinel based on the distribution of divalent cations and Fe^{3+} ions[1,2].

$ZnFe_2O_4$ is a good dielectric material with normal spinel structure[3]. Zn^{2+} ions occupy the tetrahedral sites (A), while Fe^{3+} ions occupy the octahedral sites (B). The polarization of ferrites is influenced by electron exchange between Fe^{2+} and Fe^{3+} ions, leading to localized displacement. The conduction process follows a similar mechanism, affected by the presence of ferrous ions on the octahedral sites[4]. The investigation was conducted to analyze the dielectric properties of Yb-doped $ZnFe_2O_4$ ferrite.

2 Materials and Methods

The solution combustion method was used to prepare $Zn_{1-x}Fe_2O_4$: xYb samples with varying compositions (x=0.0, 0.3, and 0.6 mol%). The stoichiometric amounts of the initial materials were dissolved separately in distilled water. The dissolved nitrates were mixed in a beaker and heated to 150 °C on a hot plate with continuous stirring at 400 rpm. Citric acid was gradually added as a fuel during stirring. When the solvent evaporates, a gel-type medium is formed. After that the sample was dried and begins to ignite itself, initiating the combustion process. The obtained material was calcined at 800 °C for 2 h. Then the pellets were made using a hydraulic press and sintered at 1000 °C for 2 h.

*Corresponding author: (E-mail: sagrawal.phy@nitrr.ac.in)

3 Results and Discussion

3.1 XRD Analysis

Figure 1 shows XRD patterns of $Zn_{1-x}Fe_2O_4$: xYb (x=0.0, 0.3, and 0.6 mol %) samples. All powder samples are polycrystalline, as indicated by multiple peaks in the diffraction patterns.

The High score plus software was used to compare the XRD data patterns in the ICSD database, which confirmed the existence of a cubic spinel structure with space group Fd-3m (Ref. code: 98-00-85866). The peaks at 32.2° and 36° are attributed to the presence of

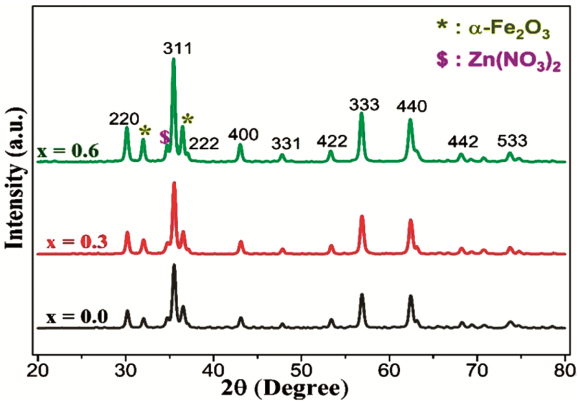

Fig. 1 — XRD patterns of $Zn_{1-x}Fe_2O_4$: xYb (x = 0.0, 0.3 and 0.6 mol%) powder sample.

α-Fe_2O_3 phase, while the peak at 34.8° is associated with $Zn(NO_3)_3$. The crystallite size of the prepared samples was determined using Scherrer's formula, as indicated in Table 1[5].

3.2 SEM Analysis

Figure 2 shows the SEM image of $Zn_{1-x}Fe_2O_4$: xYb (x = 0.6 mol%) powder sample. It can be observed that, the microstructure reveals agglomerates resembling large rocks adhering to small particles on their surface, while the morphology appears to be homogeneous and equally distributed[6].

Table 1 — Crystallographic parameters of $Zn_{1-x}Fe_2O_4$: xYb samples.

S. N.	Composition of Yb	βcosθ	Crystallite size D (nm)
1.	x = 0.0 mol %	0.00670	20.69
2.	x = 0.3 mol %	0.00808	17.16
3.	x = 0.6 mol %	0.0125	11.09

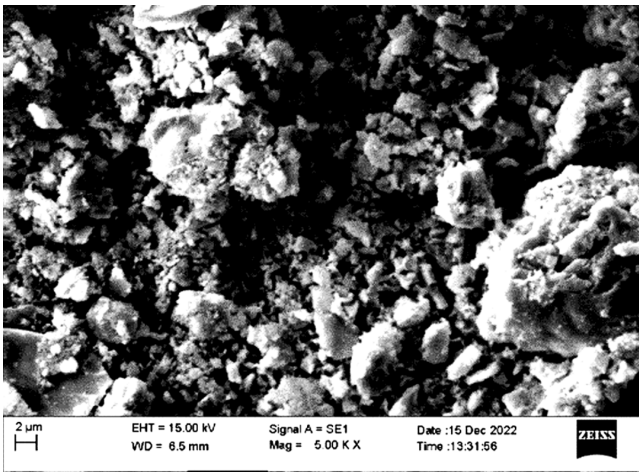

Fig. 2 — The SEM image of $Zn_{1-x}Fe_2O_4$: xYb (x = 0.6 mol%) powder sample.

3.3 Dielectric Analysis

Figure 3 shows the temperature-dependent of the dielectric constant for the prepared samples at selected frequencies. Dielectric constant increases gradually with increase in temperature in all prepared samples. At higher frequencies, its variation is nearly constant. This outcome could be a result of the polarisation, which relates to the molecule's thermal motion. As the temperature increases, the charge carrier gets thermally activated, increasing the electron exchange interactions and hence increase the dielectric constant[7,8].

The impact of temperature on the dielectric loss as shown in Fig. 4 can be explained through the phenomenon of polarization.

As temperature increases, the electrical conductivity increases as a result of the thermal activity and enhanced mobility of electrical charge carriers, following the hopping mechanism. Thus, the dielectric constant and dielectric loss increase together with the increase in dielectric polarisation[9]. This pattern keeps true for all the compositions for $Zn_{1-x}Fe_2O_4$: xYb (x=0.0, 0.3 and 0.6 mol%). The dielectric loss increases with increasing Yb (x = 0.3 mol %) substitution.

Figure 5 shows the Cole-Cole plot for the prepared samples. The plots exhibit distinct semicircular arcs and spikes, which indicate the presence of grain boundary effect in all prepared samples[10,11].

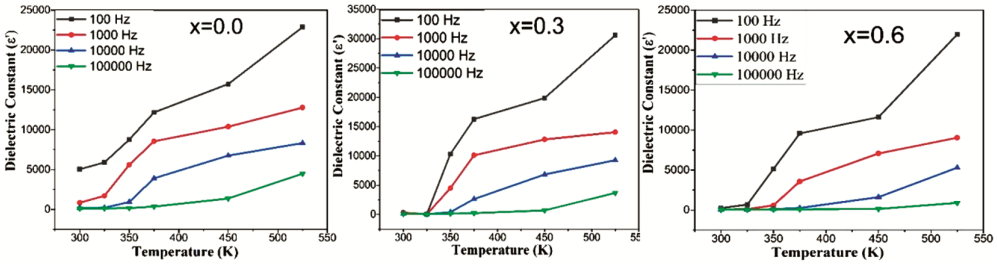

Fig. 3 — Temperature dependent dielectric constant at different frequencies for $Zn_{1-x}Fe_2O_4$: xYb (x = 0.0, 0.3 and 0.6 mol%).

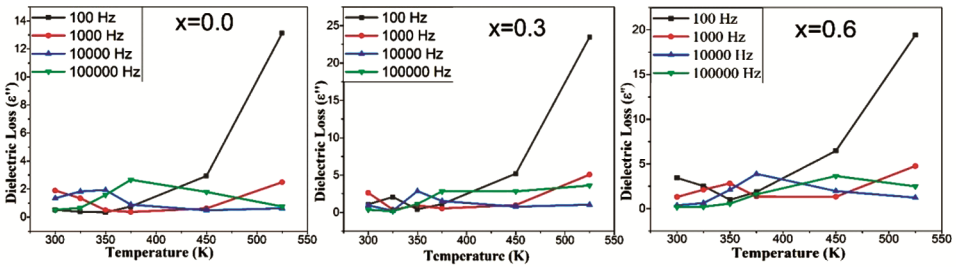

Fig. 4 — Temperature dependent dielectric loss at different frequencies for $Zn_{1-x}Fe_2O_4$: xYb (x = 0.0, 0.3 and 0.6 mol %) sample.

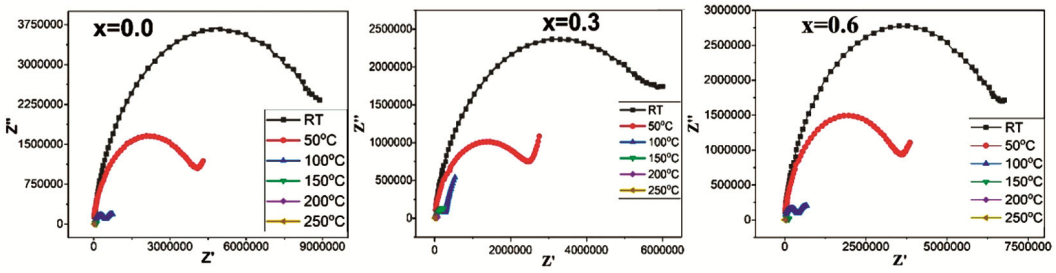

Fig. 5 — Cole-Cole plot for $Zn_{1-x}Fe_2O_4$: xYb (x = 0.0, 0.3 and 0.6 mol%) sample.

The radius of semicircle gradually decreases with increasing temperature and deviate from the centre of the real impedance axis (Z'). This observation implies the existence of a single relaxation mechanism that is non-debye nature of the samples[11].

4 Conclusion

The spinel ferrite, $Zn_{1-x}Fe_2O_4$: xYb (x=0.0, 0.3 and 0.6 mol %) were successfully synthesized via the solution combustion method. The XRD analysis revealed the formation of a cubic spinel structure with Fd-3m space group. The SEM analysis revealed agglomerates resembling large rocks adhering to small particles. The dielectric properties indicate a non-debye relaxation mechanism, with a high dielectric constant and low dielectric loss, making it a suitable choice for high-frequency applications.

Acknowledgement

The authors would like to express sincere gratitude to the NIT Raipur for providing research facility.

References

1 Qindeel R, Alonizan N H, Alghamdi E A & Awad M A, *J Sol-Gel Sci Technol*, 97 (2021) 593.
2 Thakur P,Taneja S, Chahar D, Ravelo B & Thakur A, *J Magn Magn Mater*, 530 (2021) 167925.
3 Ehrhardt H,Campbell S J & Hofmann M, *J Alloys Compd*, 339 (2002) 225.
4 Ravinder D, Reddy A V R & Mohan G R, *Mater Lett*, 52 (2002) 259.
5 Vinosha P A, Mely L A, Jeronsia J E, Krishnan S & Das S J, *Optik*, 134 (2017) 99.
6 Zhang Y, Chen Y, Kou Q, Wang Z, Han D, Sun Y, Yang J, Liu Y & Yang L, *J Mater Sci: Mater Electron,* 29 (2018) 3665.
7 Heiba Z K, Mohamed M B, Ahmed M A, Moussa M A A & Hamdeh H H, *J Alloys Compd,* 586 (2014) 773.
8 Soudani I, Brahim K B B,Oueslati A, Aydi A, Khirouni K, Benali A, Dhahri E & Valente M A, *RSC Adv,* 13 (2023) 9260.
9 Mohapatra P P, Pittal S & Dobbidi P, *J Mater Res Technol*, 9 (2020) 2992.
10 Batoo K M, Mir F A, El-sadek M S A, Shahabuddin M & Ahmed N, *J Nanoparticle Res*, 15 (2013).
11 Hafiza M N & Isa M I N, *Res J Recent Sci Res J Recent Sci*, 3 (2014) 50.